



# Antimicrobial activity of green synthesized Se nanoparticles using ginger and onion extract: a laboratory and *in silico* analysis

Fernando Martínez-Esquivias, Juan Manuel Guzmán-Flores & Alejandro Perez-Larios

To cite this article: Fernando Martínez-Esquivias, Juan Manuel Guzmán-Flores & Alejandro Perez-Larios (2022): Antimicrobial activity of green synthesized Se nanoparticles using ginger and onion extract: a laboratory and *in silico* analysis, Particulate Science and Technology, DOI: [10.1080/02726351.2022.2088432](https://doi.org/10.1080/02726351.2022.2088432)

To link to this article: <https://doi.org/10.1080/02726351.2022.2088432>



Published online: 25 Jun 2022.



Submit your article to this journal [↗](#)






View related articles [↗](#)



View Crossmark data [↗](#)



# Antimicrobial activity of green synthesized Se nanoparticles using ginger and onion extract: a laboratory and *in silico* analysis

Fernando Martínez-Esquivias<sup>a</sup> , Juan Manuel Guzmán-Flores<sup>a</sup> , and Alejandro Perez-Larios<sup>b</sup> 

<sup>a</sup>Instituto de Investigación en Biociencias, Centro Universitario de Los Altos, Universidad de Guadalajara, Tepatitlán de Morelos, Mexico;

<sup>b</sup>Laboratorio de Investigación en Materiales, Agua y Energía, Departamento de Ingenierías, Centro Universitario de Los Altos, Universidad de Guadalajara, Tepatitlán de Morelos, Mexico

## ABSTRACT

We present the green synthesis of selenium nanoparticles using onion and ginger extracts and their characterization. Subsequently, the antimicrobial effect of the nanoparticles against *Staphylococcus aureus*, *Listeria monocytogenes*, *Escherichia coli*, and *Salmonella paratyphi* was tested. Furthermore, this study implemented an *in silico* analysis using the STITCH database to generate protein-selenium interaction networks and predict altered KEGG pathways in the studied bacteria. The results showed the maximum UV-visible absorbance at approximately 550 nm confirming the synthesis of nanoparticles. Furthermore, the phenolic compounds identified to enhance the synthesis and stabilize selenium nanoparticles. The synthesized nanoparticles are spherical at about 100 nm. Selenium nanoparticles showed only an inhibitory effect on the growth of *Staphylococcus aureus*. According to *in silico* analysis, nanoparticles cause an inhibition of the growth of *Staphylococcus aureus* by an alteration in the metabolism of cysteine, methionine and arachidonic acid.

## KEYWORDS

Selenium nanoparticles; green synthesis; antimicrobial activity; *in silico* analysis; onion; ginger

## 1. Introduction

Currently, the use of nanoparticles has innovated and transformed different scientific disciplines such as the food industry, medicine and biotechnology (Chenthamara et al. 2019; Martínez-Esquivias et al. 2021b). Nanoparticles can be synthesized using various precursors and methods such as sol-gel, hydrothermal, and chemical deposition (Yang and Park 2019; Jadoun et al. 2021). However, these methods use dangerous chemical substances including reducing agents, organic solvents and stabilizing agents that could generate undesirable effects including toxicity and carcinogenicity, limiting their medical applications, in addition to generating toxic environmental effects (D. Zhang et al. 2020).

On the other hand, the green approach involves the use of protective, stabilizing and reducing agents obtained from natural sources, such as leaf, crop or fruit extracts. The components present in the extracts participate in the formation of nanoparticles, provide stabilization and increase the degree of bioavailability and biocompatibility (Khandel et al. 2018). Current studies have compared the effects of selenium nanoparticles (SeNPs) synthesized using green synthesis methods versus chemical synthesis (Anu et al. 2017; Wadhvani et al. 2017). According to Anu et al. (2017) SeNPs synthesized using aqueous extract of garlic generated less cytotoxicity in an *in vitro* study using Vero cells compared to nanoparticles synthesized by chemical synthesis method. Similarly, Wadhvani et al. (2017) compared the

anticancer effect of selenium nanoparticles synthesized by a green approach versus chemical synthesis. The results showed that the chemically synthesized nanoparticles exerted a better anticancer effect but were more toxic to non-cancerous cell lines, limiting their therapeutic application.

Phytochemicals such as terpenoids, alkaloids, phenolic compounds, flavonoids, tannins, and biomolecules such as proteins, carbohydrates, enzymes, and nucleic acids predominate in the liquid extracts of plants, leaves, or fruits (Makarov et al. 2014; Hussain et al. 2016). Research has indicated that the presence of proteins, phenolic compounds, flavonoids, or carbohydrates performs the formation of selenium nanoparticles (SeNPs) by reducing  $\text{SeO}_3^{2-}$  of the precursor salt sodium selenite ( $\text{Na}_2\text{SeO}_3$ ) for the formation of metallic/elemental selenium ( $\text{Se}^0$ ). In addition, these components can adhere to the surface of the SeNPs to provide stabilization and prevent aggregation states (Husen and Siddiqi 2014; W. Zhang et al. 2018; Shi et al. 2021; Zambonino et al. 2021). The obtained nanoparticles are spherical and their size depends on the extract composition (Akhtar, Panwar, and Yun 2013; Korde et al. 2020). Various interesting studies report that the SeNPs exhibit anticancer (Martínez-Esquivias et al. 2022), antioxidant (Kumar et al. 2020), antidiabetic (Martínez-Esquivias et al. 2021a), and antimicrobial (Martínez-Esquivias et al. 2021a) properties. In the latter respect, *in vitro* studies using SeNPs against gram-negative and gram-positive bacteria employing the agar

diffusion method were reported (Shoeibi and Mashreghi 2017; Fardsadegh et al. 2019; Salem et al. 2021).

Alternatively, STITCH is a database that offers us information on the interactions that may exist between different elements or chemical compounds in a protein network to predict the biological processes that may be affected in different organisms, including bacteria (Szklarczyk et al. 2016). Current reports have been carried out *in silico* studies using this database in order to integrate the information obtained experimentally. Verma et al. (2018) have performed an integrative analysis with this database to assess the potential toxicological effect of TiO<sub>2</sub> nanoparticles. Likewise, Cardozo et al. (2019) performed an integrative analysis using this database to elucidate the genotoxic effect of ZnO nanoparticles. Similarly, Kumari et al. (2017) evaluated the potential cytotoxic effect of CuO nanoparticles. However, to date, there are no studies that integrate the antimicrobial effect of SeNPs using this database.

The synthesis of SeNPs in presence of onion or ginger extracts is reported in the present study. The antibacterial activity of these nanoparticles against *Staphylococcus aureus*, *Listeria monocytogenes*, *Escherichia coli*, and *Salmonella paratyphi* was evaluated. To our knowledge, the use of onion extract in the synthesis of SeNPs has not been previously reported. Additionally, we performed an *in-silico* analysis through the STITCH database to learn about the KEGG pathways that could be affected by exposure to SeNPs on the bacteria under study.

## 2. Materials and methods

### 2.1. Extraction

Fresh onions and ginger, purchased from a local market, were peeled and washed first. 125 g of onion or ginger and 0.5 L of deionized water were added in a mixer. The obtained mixture was placed in 50 mL test tubes and then centrifuged at 4,500 rpm for 20 min. The obtained supernatant was filtered in a vacuum filtration system, the onion and ginger solutions were stored separately and it was ready for characterization by HPLC. Filtered extracts were stored at  $-4^{\circ}\text{C}$  for 24 h before being used for nanoparticle synthesis.

### 2.2. Extract characterization

For the identification of phenolic compounds, extract aliquots obtained from onions and gingers were analyzed by a HPLC equipment (Agilent 1200 Series HPLC System, Agilent Technologies, Santa Clara, CA, USA). The system is equipped with a matrix detector G4212-60008 UV-Vis Diode (DAD) module and coupled with an Agilent 6120 single quadrupole LC/MS, equipped with electrospray ionization with negative ionization mode interface (N2 as drying gas flow, 13.0 L/min; nebulizer pressure, 40 psi; gas drying temp. 350 C; capillary voltage, 3,500 V). 10  $\mu\text{L}$  of onion or ginger extract was first filtered using a 0.45 mm nylon membrane (Merck Millipore Ltd., Cork, Ireland), and

then automatically injected at 0.4 mL/min into a Agilent Poroshell 120 EC-C18 column (4.6 mm  $\times$  150 mm, 2.7  $\mu\text{m}$ ). The elution gradient was carried out with water containing 0.1% formic acid (Sigma-Aldrich) as a solvent A and acetonitrile (Sigma-Aldrich) as a solvent B, under the following sequence: 0 min, 5% B; 10 min, 23% B; 15 min, 50% B; 20 min, 50% B; 23–25 min, 100% B; 27 min, 5% B; 30 min, 55 B (Cárdenas-Castro et al. 2020).

### 2.3. Synthesis of SeNPs

Hundred milliliters of the onion or ginger extract and 10 g of Na<sub>2</sub>SeO<sub>3</sub> were placed in a beaker under stirring at 60  $^{\circ}\text{C}$ , 260 rpm for 3, 6 or 12 h. The color of the solution changed to red during the synthesis. After the synthesis time, a portion of the solution was placed in a quartz cuvette for UV-Vis analysis. The rest of the solution was placed in tubes of 2 mL and centrifuged at 13,000 rpm and 4  $^{\circ}\text{C}$  to remove the supernatant (extract). Successively, particles were washed tenfold with deionized water and threefold with absolute ethyl alcohol. The tubes were then dried at ambient temperature for 48 h. Finally, the samples (SeNPs) were ground in an agate mortar, and the powder obtained was used for characterization (Figure 1).

### 2.4. Characterization of SeNPs

Absorbance spectra were obtained in a UV-Vis spectrophotometer (Shimadzu UV-2600, Tokyo, Japan). The morphology of the SeNPs was determined by scanning electron microscopy (SEM), (Tescan MIRA3 LMU, London, the UK at 20 kV). Additional features of the nanoparticles were determined by transmission electron microscopy (TEM) (JOEL JEM 1010 with an acceleration voltage of 100 kV). The X-ray diffraction (XRD) patterns were obtained in a Empyrean Diffractometer, Malvern Panalytical, Almelo, the Netherland, equipped with Cu K $\alpha$  radiation ( $\lambda = 0.154\text{ nm}$ ) in a range of 10–90  $^{\circ} 2\theta$  and 4 s/step. ATR-FTIR spectroscopy (Nicolet iS5, ThermoFisher Scientific, Tokyo, Japan) was also used for characterization. The spectra were acquired in a range of 400–4,000  $\text{cm}^{-1}$  with 24 scans per spectrum and a resolution of 4  $\text{cm}^{-1}$ .

### 2.5. Antibacterial activity of SeNPs

Based on a previous report on the antibacterial activity of SeNPs (Shoeibi and Mashreghi 2017), our nanoparticles were evaluated against *Staphylococcus aureus* (ATCC 33862), *Listeria monocytogenes* (ATCC 15313), *Escherichia coli* (ATCC 8739), and *Salmonella paratyphi* (ATCC 9150) by the disk diffusion method. Bacteria of 10<sup>8</sup> CFU/mL were uniformly spread cultivated in Petri dishes provided with a Muller Hinton agar medium. Subsequently, sterile paper disks of 6 mm in diameter, previously impregnated with nanoparticles (25, 50, and 100  $\mu\text{g}/\text{mL}$ ) were placed on the agar plate. Additionally, sterile paper disks were impregnated with the onion or ginger extract. Disks of Gentamicin (10  $\mu\text{g}$ ) were used as the positive control (C+), and disks

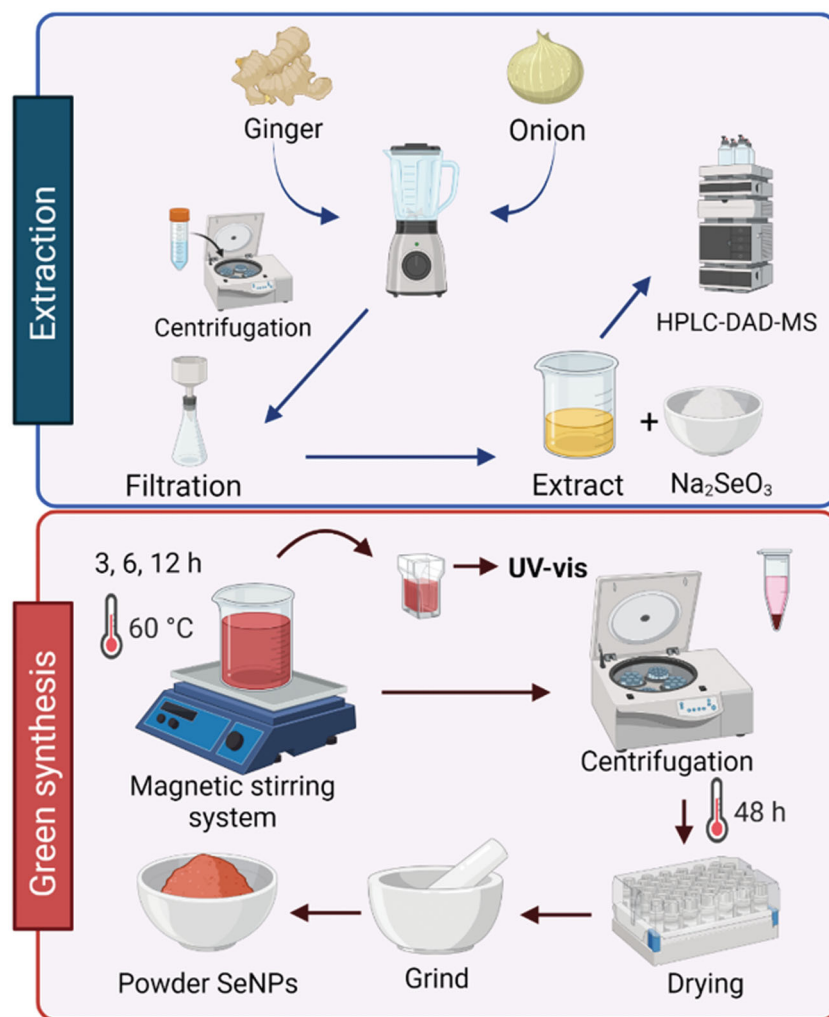


Figure 1. Preparation of extracts and synthesis of SeNPs.

impregnated with sterile double distilled water as the negative control (C-). All plates were incubated at 37 °C for 24 h. The antimicrobial activity was determined by measuring the zone of inhibition around the disk in millimeters. All experiments were performed in triplicate.

## 2.6. *In silico* analysis

For the *in silico* analysis, we worked on the STITCH database (<http://stitch.embl.de/>) to generate interaction networks between selenium and proteins for each of the bacteria studied. Additionally, possible KEEG pathways affected by selenium exposure were predicted (Szklarczyk et al. 2016). For protein-selenium interaction networks, a minimum interaction score of 0.400 was considered with no more than 10 interactions shown. For the KEGG analysis, a False Discovery Rate (FDR) < 0.05 was considered.

## 2.7. Statistical analysis

The bacterial inhibition was expressed as the mean ± the standard deviation (SD). The statistical significance between groups was determined by the Kruskal–Wallis analysis, following the Post-Hoc testing.

Table 1. Phenolic compounds present in onion and ginger extracts identified by HPLC-DAD-MS.

Compound	$R_t$	$m/z$ [-]
Onion extract		
Quercetin	17.53	301
Ginger extract		
5-Acetoxy-1,7-bis (4-hydroxy-3-methoxyphenyl) heptan-3-one	18.71	357.21
6-Gingerdiol	11.213	261.21
6-Gingerol	4.01	277.21
10-Gingerol	22.731	333.28
Acetoxy-10-gingerol	23.486	333.28
5,7,3',4'-Tetramethoxyflavone	16.6	381.07
3,5,7,3',4'-Pentamethoxyflavone	20.50	411.09

## 3. Results and discussion

### 3.1. Extract characterization

Quercetin and gingerols reported in Table 1 were the phenolic compounds identified by HPLC-DAD-MS in onion and ginger extracts, respectively. These findings have also been recorded by Cecchi et al. (2020) and Asamenew et al. (2019). The phenolic compounds participate as reducing and stabilizing agents during the synthesis of SeNPs. In addition, they prevent aggregation of particles and impart antioxidant properties (Mellinas, Jiménez, and Garrigós 2019).

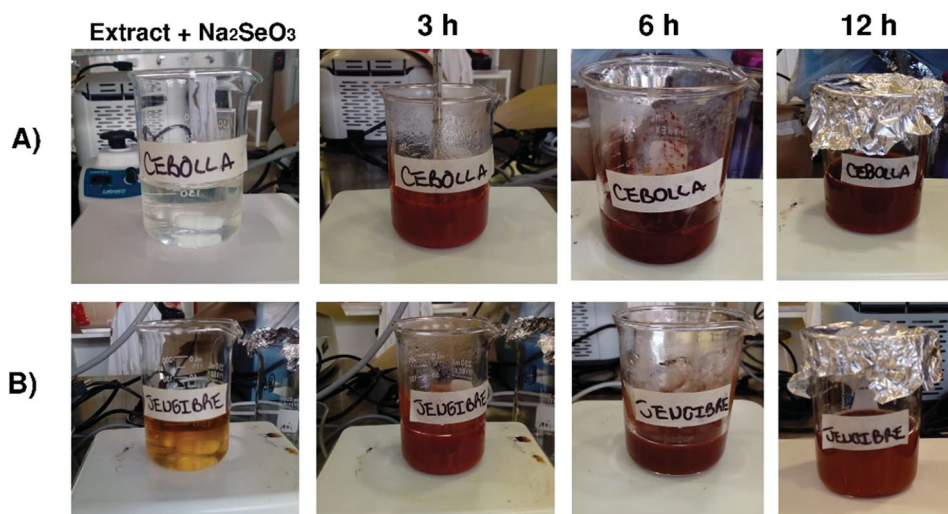
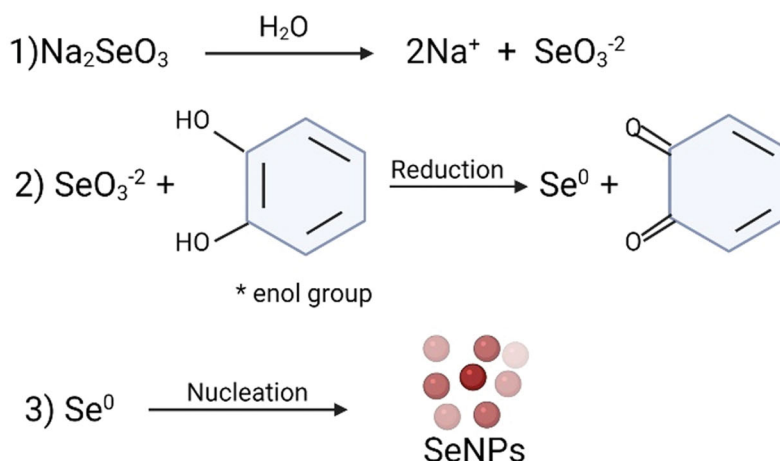


Figure 2. Color changes of onion (A) and ginger (B) extracts.



\*Enol group of phenolic compounds of the extracts break O-H bond that releases an electron to reduce Se.

Figure 3. Proposed mechanism of SeNPs synthesis.

### 3.2. Synthesis of SeNPs

During the synthesis of particles, the color of the extract solutions changed from colorless (onion) and yellow (ginger) to dark red (Figure 2). This change in color is related to the formation of SeNPs (Husen and Siddiqi 2014) and resulted from the reduction of selenium ions to  $\text{Se}^0$  in presence of phenolic compounds (Hussain et al. 2016). Figure 3 Show possible mechanism of SeNPs synthesis in the presence of phenolic compounds.

### 3.3. Characterization of SeNPs

The formation of SeNPs was also confirmed using UV-vis spectroscopy between 400 and 800 nm (Figure 4). The absorbance detected at about 550 nm is indicative of the surface plasmon resonance (SPR) band. Similar absorbance references were taken by other authors for the formation of SeNPs in the presence of *Pseudomonas aeruginosa* (Kora

and Rastogi 2016), *Trichoderma sp* (Diko et al. 2020), and *Magnusiomyces ingens* (Lian et al. 2019). Our results indicate that the phenolic compounds present in the natural extracts from onion and ginger act as reducing agents and could be a viable alternative for the synthesis of SeNPs. In addition, it can be seen that there are differences between the absorption spectra of the SeNPs synthesized using onion and ginger extract. These differences can be explained based on the atomic structure of the synthesized SeNPs (Kora and Rastogi 2016).

SEM analysis showed a spherical morphology of the synthesized SeNPs (Figure 5). For its part, the TEM analysis showed nanoparticles with a diameter of approximately 90 nm, except those synthesized in the presence of onion extract at 12 h, which are approximately 114 nm (Figure 6). These results are in agreement with previous reports regarding SeNPs synthesized with ginger extract. Menon et al. (2019) reported particle sizes from 100 to 150 nm, whereas Zahran, Elsonbaty, and Moawed (2017) obtained particles in

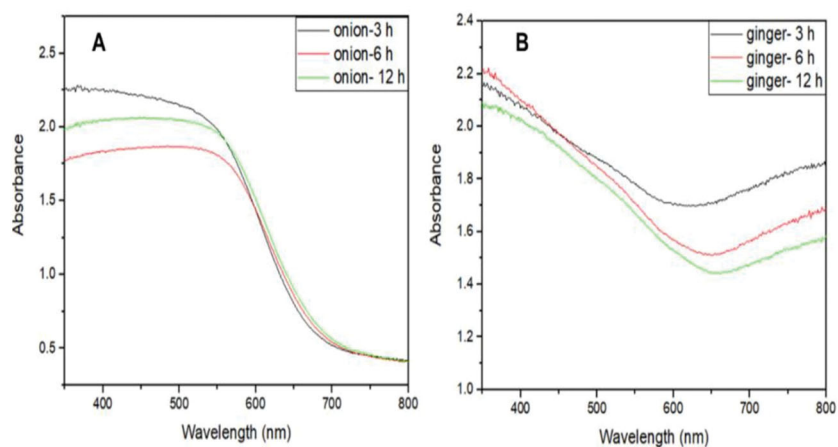


Figure 4. UV-Vis absorbance spectra of SeNPs synthesized in presence of onion (A) and ginger (B) extracts.

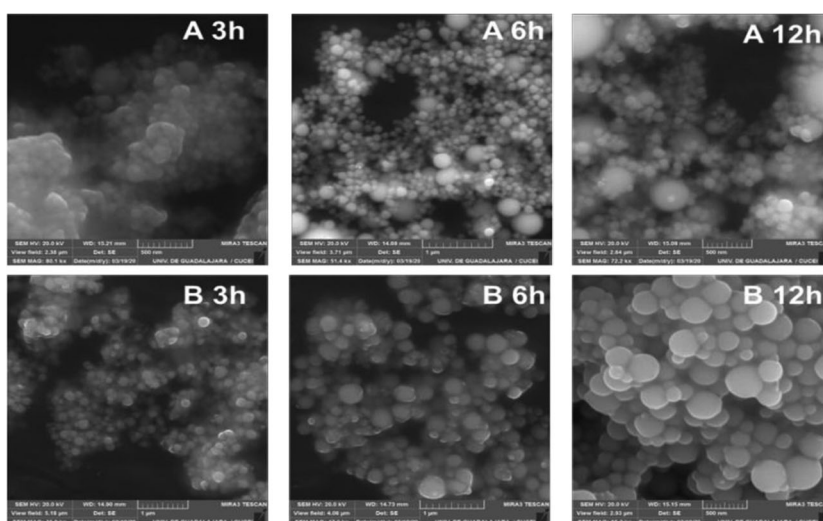


Figure 5. SEM images of SeNPs synthesized in presence of onion (A) and ginger (B) extracts.

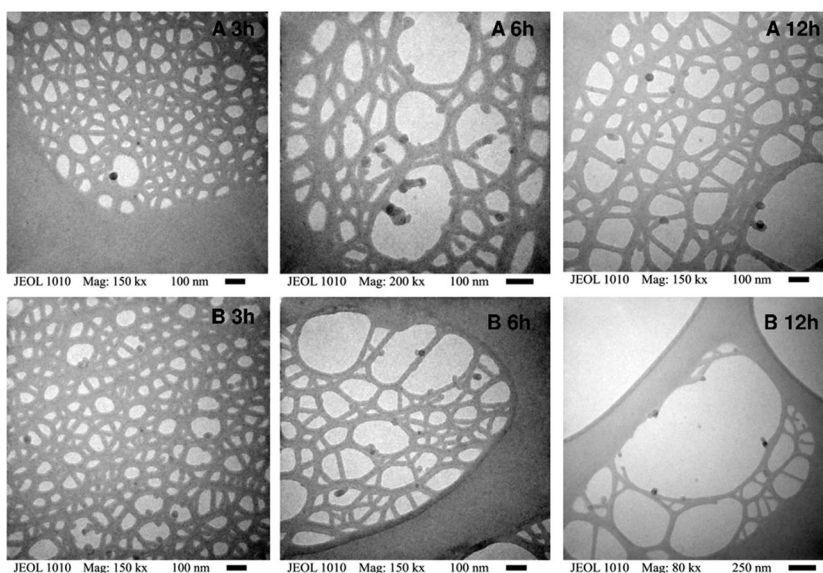
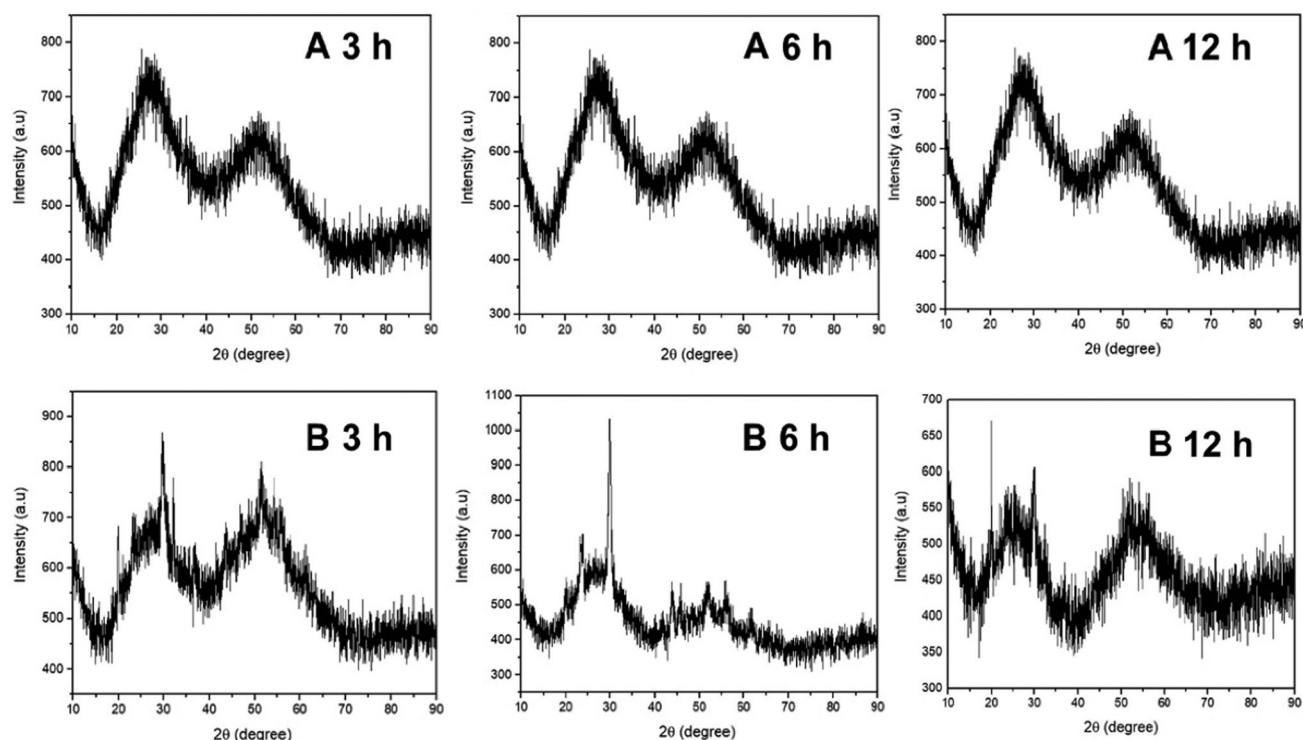


Figure 6. TEM images of SeNPs synthesized in presence of onion (A) and ginger (B) extracts.



**Figure 7.** XRD spectra of SeNPs synthesized in presence of onion (A) and ginger (B) extracts.

the range of 10–30 nm. In addition, Mulla et al. (2020), Liang et al. (2020), W. Zhang et al. (2018), and Anu et al. (2017) have also studied the synthesis of SeNPs in the presence of *Azadirachta indica*, *Oscimum tenuiflorum*, a polysaccharide from *Lycium barbarum* and *Allium sativum*, and reported particle sizes of 153–278, 15–20, 83–160, and 40–110 nm, respectively. These variations are due to differences in the precursors and synthesis conditions (Akhtar, Panwar, and Yun 2013).

The XRD patterns of the SeNPs synthesized using onion extract (Figure 7(A)) show broad diffraction signals, which are indicative of amorphous structures. The diffractions are assigned to the trigonal phase of selenium, with  $a = 4.362 \text{ \AA}$  and  $c = 4.958 \text{ \AA}$  according to the JCPDS, file No. 06-362. Amorphous structures related to SeNPs have also been reported (Chen et al. 2009; Alagesan and Venugopal 2019). On the other hand, the SeNPs synthesized using ginger extract (Figure 7(B)) show sharp peaks at  $2\theta$  values at  $20^\circ$  and  $30^\circ$  approximately, which suggests a crystalline structure according to file No. 06-362, which is consistent with what has been reported by Wadhvani et al. (2017). However, other characteristic peaks of the crystalline structures are not appreciated due to the noise generated by the organic compounds present in the synthesized SeNPs (Vikneshan et al. 2020).

The FTIR spectra as function of extract and synthesis time are shown in Figure 8. The FTIR spectra of the nanoparticles synthesized from the onion extract (Figure 8(A)) show peak at  $965 \text{ cm}^{-1}$  is assigned to carbohydrate functional groups, and those at about 2,979, 2,346, 1,636 and  $1,145 \text{ cm}^{-1}$  to methylene CH asym/sym stretching band, C=N=O asymmetric stretching, and the latter two to the amide groups I, respectively. The functional signals result

from lipids, proteins, carbohydrates, and polyphenols present in the extracts. In addition, the absorption peaks  $2,933$ ,  $2,346$  and  $1,636 \text{ cm}^{-1}$  become narrower, their intensity decreases and they move to low frequency regions according to the synthesis time, these structural changes are due to the fact that these functional groups participate in the reduction and stabilization of nanoparticles Abboud et al. (2013). Figure 8(B) also shows the FTIR spectra of the SeNPs synthesized in presence ginger extract. Similarly, the signals at about  $2,984$  and  $2,882 \text{ cm}^{-1}$  are attributed to methylene CH asym/sym stretching mode, that at about  $2,324 \text{ cm}^{-1}$  to C=N=O asymmetric stretch, those at 1,658, 1,269, 1,030 and  $738 \text{ cm}^{-1}$  to the vibrations of the amide group I, the skeleton C-C, the stretching of the CN group of the primary amines and to the torsional CH deformation of the polysaccharide ring, respectively.

The changes in the absorption of the resulted species observed in the FTIR spectra are a clear indication of the oxidation-reduction reactions occurring throughout the synthesis process. In addition, it demonstrates that onion and ginger extracts are suitable for the synthesis of SeNPs (Zahran, Elsonbaty, and Moawed 2017; Menon et al. 2019).

### 3.4. Antibacterial activity

Figure 9 shows the zones of inhibition against *Staphylococcus aureus*. Our results indicate that SeNPs decreased the growth of *Staphylococcus aureus*, showing an insignificant dose-dependent effect when the Kruskal-Wallis test was applied (Figure 10). It is worth commenting that the extracts alone did not show any antimicrobial activity and as a consequence, the activity was only attributed to the

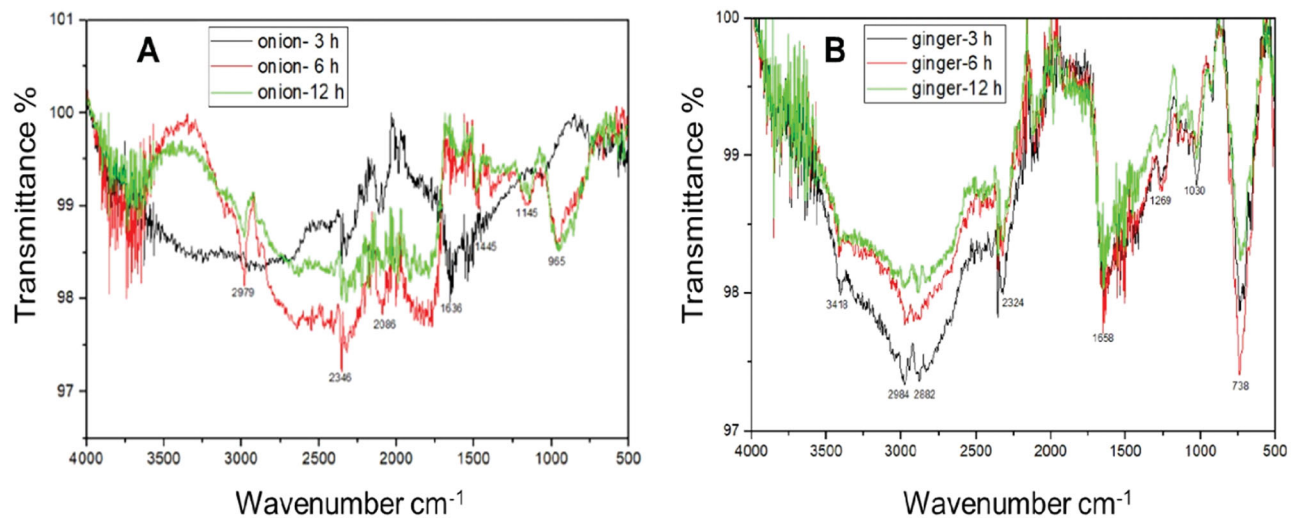


Figure 8. FTIR spectra of SeNPs synthesized in presence of onion (A) and ginger (B) extracts.

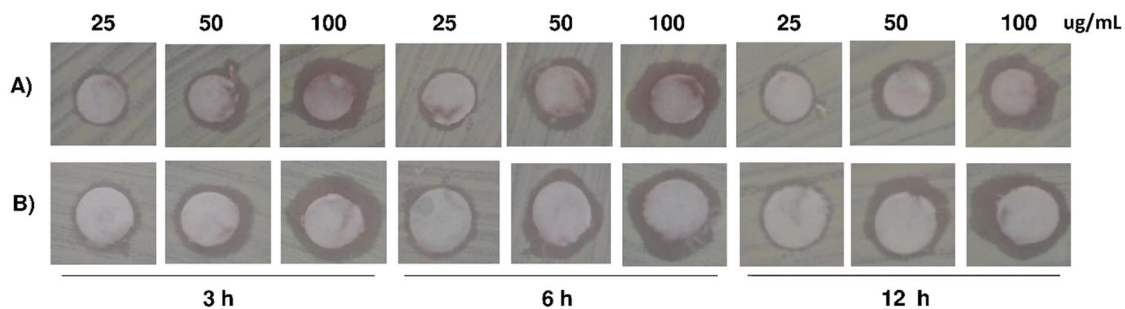


Figure 9. Zones of inhibition of SeNPs synthesized in presence of onion (A) and ginger (B) extracts against *Staphylococcus aureus*.

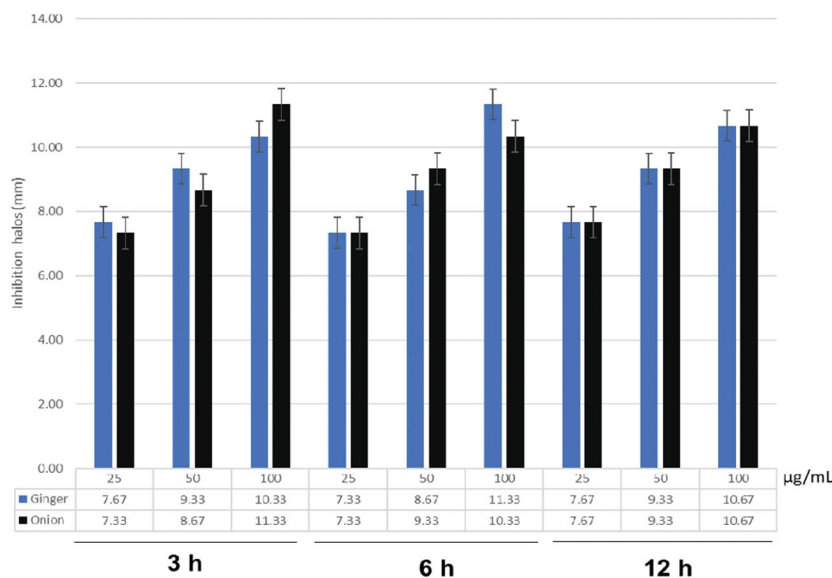
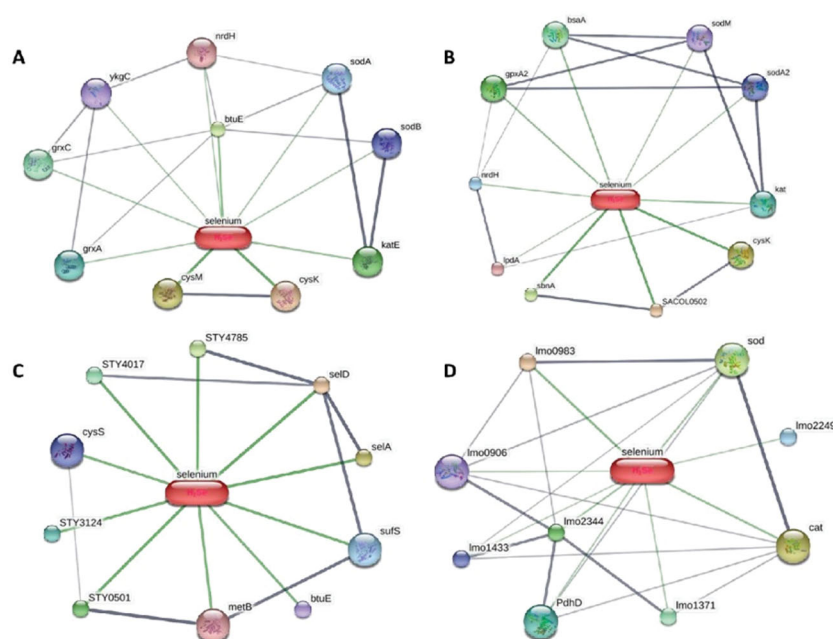


Figure 10. Antimicrobial activity of the SeNPs against *Staphylococcus aureus*.

presence of the SeNPs. Other studies have reported similar effects. SeNPs showed activity against *Staphylococcus aureus* and resistance to the growth of *Bacillus subtilis*, *Escherichia coli*, and *Pseudomonas aeruginosa* (Shoeibi and Mashreghi 2017). Vahdati and Tohidi Moghadam (2020) found that SeNPs ( $35.6 \pm 7.5$  nm) efficiently reduced the growth of *Staphylococcus aureus* (MIC =  $82 \mu\text{g/mL}$ ) and showed

resistance to the growth of *Escherichia coli*. Guisbiers et al. (2016) also reported that SeNPs ( $115 \pm 38$  nm) exhibited a significant greater inhibition effect on the growth of *Staphylococcus aureus* than on *Escherichia coli*. Salem et al. (2021) reported that the SeNPs synthesized in presence of *Penicillium corylophilum* fungus, showed antibacterial activity against gram-positive and gram-negative bacteria





**Figure 11.** Interaction networks of selenium and proteins to *Escherichia coli* (A), *Staphylococcus aureus* (B), *Salmonella* (C), *Listeria monocytogenes* (D). Stronger associations are represented by thicker lines. Protein-protein interactions are shown in gray, chemical-protein interactions in green and interactions between chemicals in red.

**Table 2.** KEGG enrichment pathways deregulated by selenium exposure.

#Pathway ID	Pathway description	FDR	Molecules involved in the metabolic pathway
<i>Staphylococcus aureus</i>			
270	Cysteine and methionine metabolism	0.00309	SACOL0502, cysK, sbnA
590	Arachidonic acid metabolism	0.00309	bsaA, gpxA2
1120	Microbial metabolism in diverse environments	0.00309	SACOL0502, cysK, kat, lpdA, sbnA
480	Glutathione metabolism	0.00818	bsaA, gpxA2
920	Sulfur metabolism	0.0112	cysK, sbnA
<i>Salmonella</i>			
450	Selenocompound metabolism	7.55E-09	STY4785, metB, selA, selD, sufS
970	Aminoacyl-tRNA biosynthesis	0.00145	STY4785, cysS, selA
<i>Listeria monocytogenes</i>			
480	Glutathione metabolism	0.00011	Imo0906, Imo0983, Imo1433
20	Citrate cycle (TCA cycle)	0.0166	PdhD, Imo1371
280	Valine, leucine and isoleucine degradation	0.0166	PdhD, Imo1371

(*Staphylococcus aureus*, *Bacillus subtilis*, *Escherichia coli*, and *Pseudomonas aeruginosa*). The inhibition halos were 33.3, 23.6, 22.6, and 20 mm, respectively, with a 150 µg of nanoparticles/mL. Menon et al. (2019) reported that the SeNPs synthesized using ginger extract effectively suppressed the growth of gram-negative bacteria *Proteus* sp, *Serratia* sp, and *Escherichia coli* at a concentration of 100 µg of nanoparticles/mL. The inhibition halos were 20, 17, and 12 mm, respectively. In contrast, the *Staphylococcus aureus* and *Bacillus subtilis* inhibition halos were 7 and 5 mm, respectively.

### 3.5. In silico analysis

Figure 11 shows the interaction networks between proteins and selenium that were predicted in the STITCH database for the bacteria *Escherichia coli*, *Staphylococcus aureus*, *Salmonella*, and *Listeria monocytogenes*. Table 2 shows the KEGG pathways that could be affected by exposure to selenium. According to the results of the *in silico* analysis of

KEGG pathways (Table 2), selenium could affect the metabolism of cysteine, methionine, arachidonic acid and sulfur for *Staphylococcus aureus*. However, the pathways in which selenium is involved in *Salmonella* are selenocompound metabolism and aminoacyl-tRNA biosynthesis. Meanwhile, selenium can affect pathways related to glutathione metabolism and valine, leucine, and isoleucine degradation in *Listeria monocytogenes*. For *Escherichia coli*, the analysis showed no KEGG pathways that could be affected.

By relating the results of the *in vitro* to the *in silico* analysis, we could infer that the exposure to SeNPs inhibited the growth of *Staphylococcus aureus* due to an alteration in the metabolism of cysteine and methionine. In the literature, it has been mentioned that exposure to SeNPs generates an antimicrobial effect on the generation of reactive oxygen species (ROS) (Martínez-Esquivias et al. 2021a). Both amino acids can be oxidized by ROS and cause enzyme inhibition (Gaupp, Ledala, and Somerville 2012). These results are interesting since methionine metabolism has been considered a target for drug development against.

*Staphylococcus aureus* (Schoenfelder et al. 2013). On the other hand, an alteration in the metabolism of arachidonic acid could generate a toxic effect on *Staphylococcus aureus* due to a lipid peroxidation mechanism. This route has also been suggested for developing of new agents against *Staphylococcus aureus* (Beavers et al. 2019).

However, the exposure of SeNPs did not show inhibition in the growth of *Salmonella paratyphi* and *Listeria monocytogenes*, so we could not relate the *in vitro* analysis with the *in silico* analysis. However, the biosynthesis of aminoacyl-tRNA and the citrate cycle are considered targets to produce an antimicrobial effect that should be studied in greater depth in future works (Martínez and Rojo 2011; Chopra and Reader 2014). Additionally, we must emphasize that the results obtained from the *in silico* analysis should be experimentally corroborated in future work.

### 3.5.1. Perspectives

Future works will evaluate the antioxidant effect and the cellular cytotoxicity of the synthesized SeNPs.

## 4. Conclusions

Green synthesis of selenium nanoparticles using onion and ginger extracts and their characterization is herein reported. In addition, their antimicrobial effect against *Staphylococcus aureus*, *Listeria monocytogenes*, *Escherichia coli*, and *Salmonella paratyphi* was evaluated. Our results indicate that the natural compounds present in the extracts were capable to reduce the  $\text{SeO}_3^{-2}$  species to form metallic selenium nanoparticles. The selenium nanoparticles are spherical of about 100 nm in diameter. The microbial inhibition test showed activity against *Staphylococcus aureus* and resistance against *Escherichia coli*, *Salmonella paratyphi*, and *Listeria monocytogenes* for all SeNPs. The advantages of using these extracts compared to the methods that use ascorbic acid as a reducing agent are that the extracts provide us with natural components that act as reducing agents for the formation of SeNPs, in addition, to providing stabilization and avoiding states of aggregation. In contrast, methods using ascorbic acid only provide a reducing environment for the synthesis of nanoparticles but it is necessary to add a stabilizing agent. In addition, we must mention that although the SeNPs did not present potent antibacterial activity, they could be functionalized with antimicrobial substances to improve their activity in future works. Finally, we relate the results of the *in vitro* with the *in silico* analysis in which we were able to attribute that the inhibition in the growth of *Staphylococcus aureus* is due to an alteration in the metabolism of cysteine, methionine and arachidonic acid, considered targets for developing of agents against *Staphylococcus aureus*.

## Acknowledgments

F M-E is receiving a doctoral scholarship from CONACYT.

## Disclosure statement

No potential conflict of interest was reported by the author(s).

## ORCID

Fernando Martínez-Esquivias  <http://orcid.org/0000-0002-5059-3153>  
 Juan Manuel Guzmán-Flores  <http://orcid.org/0000-0002-4673-112X>  
 Alejandro Perez-Larios  <http://orcid.org/0000-0001-8656-5667>

## References

- Abboud, Y., A. Eddahbi, A. El Bouari, H. Aitenneite, K. Brouzi, and J. Mouslim. 2013. Microwave-assisted approach for rapid and green phyto-synthesis of silver nanoparticles using aqueous onion (*Allium cepa*) extract and their antibacterial activity. *Journal of Nanostructure in Chemistry* 3 (1):84. doi:10.1186/2193-8865-3-84.
- Akhtar, M. S., J. Panwar, and Y.-S. Yun. 2013. Biogenic synthesis of metallic nanoparticles by plant extracts. *ACS Sustainable Chemistry & Engineering* 1 (6):591–602. doi:10.1021/sc300118u.
- Alagesan, V., and S. Venugopal. 2019. Green synthesis of selenium nanoparticle using leaves extract of *Withania Somnifera* and its biological applications and photocatalytic activities. *BioNanoScience* 9 (1):105–16. doi:10.1007/s12668-018-0566-8.
- Anu, K., G. Singaravelu, K. Murugan, and G. Benelli. 2017. Green-synthesis of selenium nanoparticles using garlic cloves (*Allium sativum*): Biophysical characterization and cytotoxicity on vero cells. *Journal of Cluster Science* 28 (1):551–63. doi:10.1007/s10876-016-1123-7.
- Asamnew, G., H.-W. Kim, M.-K. Lee, S.-H. Lee, Y. J. Kim, Y.-S. Cha, S. M. Yoo, and J.-B. Kim. 2019. Characterization of phenolic compounds from normal ginger (*Zingiber officinale* Rosc.) and black ginger (*Kaempferia parviflora* Wall.) using UPLC–DAD–QToF–MS. *European Food Research and Technology* 245 (3):653–65. doi:10.1007/s00217-018-3188-z.
- Beavers, W. N., A. J. Monteith, V. Amarnath, R. L. Mernaugh, L. J. Roberts, W. J. Chazin, S. S. Davies, and E. P. Skaar. 2019. Arachidonic acid kills *Staphylococcus aureus* through a lipid peroxidation mechanism. *mBio* 10 (5):e01333–19. doi:10.1128/mBio.01333-19.
- Cárdenas-Castro, A. P., E. Alvarez-Parrilla, E. Montalvo-González, J. A. Sánchez-Burgos, K. Venema, and S. G. Sáyago-Ayerdi. 2020. Stability and anti-topoisomerase activity of phenolic compounds of *Capsicum annum* “serrano” after gastrointestinal digestion and *in vitro* colonic fermentation. *International Journal of Food Sciences and Nutrition* 71 (7):826–38. doi:10.1080/09637486.2020.1734542.
- Cardozo, T. R., R. F. De Carli, A. Seeber, W. H. Flores, J. A. N. da Rosa, Q. S. G. Kotzal, M. Lehmann, F. R. da Silva, and R. R. Dihil. 2019. Genotoxicity of zinc oxide nanoparticles: An *in vivo* and *in silico* study. *Toxicology Research* 8 (2):277–86. doi:10.1039/c8tx00255j.
- Cecchi, L., F. Ieri, P. Vignolini, N. Mulinacci, and A. Romani. 2020. Characterization of volatile and flavonoid composition of different cuts of dried onion (*Allium cepa* L.) by HS-SPME-GC-MS, HS-SPME-GC × GC-TOF and HPLC-DAD. *Molecules* 25 (2):408. doi:10.3390/molecules25020408.
- Chen, Z., Y. Shen, A. Xie, J. Zhu, Z. Wu, and F. Huang. 2009. L-cysteine-assisted controlled synthesis of selenium nanospheres and nanorods. *Crystal Growth & Design* 9 (3):1327–33. doi:10.1021/cg800398b.
- Chenthamara, D., S. Subramaniam, S. G. Ramakrishnan, S. Krishnaswamy, M. M. Essa, F.-H. Lin, and M. W. Qoronfleh. 2019. Therapeutic efficacy of nanoparticles and routes of administration. *Biomaterials Research* 23 (1):20. doi:10.1186/s40824-019-0166-x.
- Chopra, S., and J. Reader. 2014. TRNAs as antibiotic targets. *International Journal of Molecular Sciences* 16 (1):321–49. doi:10.3390/ijms16010321.
- Diko, C. S., H. Zhang, S. Lian, S. Fan, Z. Li, and Y. Qu. 2020. Optimal synthesis conditions and characterization of selenium nanoparticles

- in *Trichoderma* sp. WL-Go culture broth. *Materials Chemistry and Physics* 246 (May):122583. doi:10.1016/j.matchemphys.2019.122583.
- Fardsadegh, B., H. Vaghari, R. Mohammad-Jafari, Y. Najian, and H. Jafarizadeh-Malmiri. 2019. Biosynthesis, characterization and antimicrobial activities assessment of fabricated selenium nanoparticles using *Pelargonium zonale* leaf extract. *Green Processing and Synthesis* 8 (1):191–8. doi:10.1515/gps-2018-0060.
- Gaupp, R., N. Ledala, and G. A. Somerville. 2012. Staphylococcal response to oxidative stress. *Frontiers in Cellular and Infection Microbiology* 2:33. doi:10.3389/fcimb.2012.00033.
- Guisbiers, G., Q. Wang, E. Khachatryan, L. C. Mimun, R. Mendoza-Cruz, P. Larese-Casanova, T. J. Webster, and K. L. Nash. 2016. Inhibition of *E. coli* and *S. aureus* with selenium nanoparticles synthesized by pulsed laser ablation in deionized water. *International Journal of Nanomedicine* 11 (August):3731–6. doi:10.2147/IJN.S106289.
- Husen, A., and K. S. Siddiqi. 2014. Plants and microbes assisted selenium nanoparticles: characterization and application. *Journal of Nanobiotechnology* 12 (August):28. doi:10.1186/s12951-014-0028-6.
- Hussain, I., N. B. Singh, A. Singh, H. Singh, and S. C. Singh. 2016. Green synthesis of nanoparticles and its potential application. *Biotechnology Letters* 38 (4):545–60. doi:10.1007/s10529-015-2026-7.
- Jadoun, S., R. Arif, N. K. Jangid, and R. K. Meena. 2021. Green synthesis of nanoparticles using plant extracts: A review. *Environmental Chemistry Letters* 19 (1):355–74. doi:10.1007/s10311-020-01074-x.
- Khandel, P., R. Kumar Yadaw, D. Kumar Soni, L. Kanwar, and S. K. Shahi. 2018. Biogenesis of metal nanoparticles and their pharmacological applications: Present status and application prospects. *Journal of Nanostructure in Chemistry* 8 (3):217–54. doi:10.1007/s40097-018-0267-4.
- Kora, A. J., and L. Rastogi. 2016. Biomimetic synthesis of selenium nanoparticles by *Pseudomonas aeruginosa* ATCC 27853: An approach for conversion of selenite. *Journal of Environmental Management* 181 (October):231–6. doi:10.1016/j.jenvman.2016.06.029.
- Korde, P., S. Ghotekar, T. Pagar, S. Pansambal, R. Oza, and D. Mane. 2020. Plant extract assisted eco-benevolent synthesis of selenium nanoparticles – A review on plant parts involved, characterization and their recent applications. *Journal of Chemical Reviews* 2 (3): 157–68. doi:10.22034/jcr.2020.106601.
- Kumar, A., B. Prasad, J. Manjhi, and K. S. Prasad. 2020. Antioxidant activity of selenium nanoparticles biosynthesized using a cell-free extract of *Geobacillus*. *Toxicological & Environmental Chemistry* 102 (10):556–67. doi:10.1080/02772248.2020.1829623.
- Kumari, P., P. Kumar Panda, E. Jha, K. Kumari, K. Nisha, M. Anwar Mallick, and S. K. Verma. 2017. Mechanistic insight to ROS and apoptosis regulated cytotoxicity inferred by green synthesized CuO nanoparticles from *Calotropis gigantea* to embryonic zebrafish. *Scientific Reports* 7 (1):16284. doi:10.1038/s41598-017-16581-1.
- Lian, S., C. Sekyerebea Diko, Y. Yan, Z. Li, H. Zhang, Q. Ma, and Y. Qu. 2019. Characterization of biogenic selenium nanoparticles derived from cell-free extracts of a novel yeast *Magnusiomyces ingens*. *3 Biotech* 9 (6):221. doi:10.1007/s13205-019-1748-y.
- Liang, T., X. Qiu, X. Ye, Y. Liu, Z. Li, B. Tian, and D. Yan. 2020. Biosynthesis of selenium nanoparticles and their effect on changes in urinary nanocrystallites in calcium oxalate stone formation. *3 Biotech* 10 (1):23. doi:10.1007/s13205-019-1999-7.
- Makarov, V. V., A. J. Love, O. V. Sinitsyna, S. S. Makarova, I. V. Yaminsky, M. E. Taliansky, and N. O. Kalinina. 2014. “Green” nanotechnologies: Synthesis of metal nanoparticles using plants. *Acta Naturae* 6 (1):35–44. doi:10.32607/20758251-2014-6-1-35-44.
- Martínez, J. L., and F. Rojo. 2011. Metabolic regulation of antibiotic resistance. *FEMS Microbiology Reviews* 35 (5):768–89. doi:10.1111/j.1574-6976.2011.00282.x.
- Martínez-Esquivias, F., M. Gutiérrez-Angulo, A. Pérez-Larios, J. Sánchez-Burgos, J. Becerra-Ruiz, and J. M. Guzmán-Flores. 2022. Anticancer activity of selenium nanoparticles in vitro studies. *Anti-Cancer Agents in Medicinal Chemistry* 22 (9):1658–73. September. doi:10.2174/1871520621666210910084216.
- Martínez-Esquivias, F., J. M. Guzmán-Flores, A. Pérez-Larios, N. González Silva, and J. S. Becerra-Ruiz. 2021a. A review of the antimicrobial activity of selenium nanoparticles. *Journal of Nanoscience and Nanotechnology* 21 (11):5383–98. doi:10.1166/jnn.2021.19471.
- Martínez-Esquivias, F., J. M. Guzmán-Flores, A. Pérez-Larios, J. L. Rico, and J. S. Becerra-Ruiz. 2021b. A review of the effects of gold, silver, selenium, and zinc nanoparticles on diabetes mellitus in murine models. *Mini Reviews in Medicinal Chemistry* 21 (14):1798–812. doi:10.2174/1389557521666210203154024.
- Mellinas, C., A. Jiménez, and M. D. C. Garrigós. 2019. Microwave-assisted green synthesis and antioxidant activity of selenium nanoparticles using *Theobroma cacao* L. bean shell extract. *Molecules* 24 (22):4048. doi:10.3390/molecules24224048.
- Menon, S., K. Shrudhi Devi, H. Agarwal, and V. K. Shanmugam. 2019. Efficacy of biogenic selenium nanoparticles from an extract of ginger towards evaluation on anti-microbial and anti-oxidant activities. *Colloid and Interface Science Communications* 29 (March):1–8. doi:10.1016/j.colcom.2018.12.004.
- Mulla, N. A., S. V. Otari, R. A. Bohara, H. M. Yadav, and S. H. Pawar. 2020. Rapid and size-controlled biosynthesis of cyto-compatible selenium nanoparticles by *Azadirachta indica* leaves extract for antibacterial activity. *Materials Letters* 264 (April):127353. doi:10.1016/j.matlet.2020.127353.
- Salem, S. S., M. M. G. Fouda, A. Fouda, M. A. Awad, E. M. Al-Olayan, A. A. Allam, and T. I. Shaheen. 2021. Antibacterial, cytotoxicity and larvicidal activity of green synthesized selenium nanoparticles using *Penicillium corylophilum*. *Journal of Cluster Science* 32 (2):351–61. doi:10.1007/s10876-020-01794-8.
- Schoenfelder, S. M. K., G. Marincola, T. Geiger, C. Goerke, C. Wolz, and W. Ziebuhr. 2013. Methionine biosynthesis in *Staphylococcus aureus* is tightly controlled by a hierarchical network involving an initiator tRNA-specific T-box riboswitch. *PLoS Pathogens* 9 (9): e1003606. doi:10.1371/journal.ppat.1003606.
- Shi, X.-D., Y.-Q. Tian, J.-L. Wu, and S.-Y. Wang. 2021. Synthesis, characterization, and biological activity of selenium nanoparticles conjugated with polysaccharides. *Critical Reviews in Food Science and Nutrition* 61 (13):2225–12. doi:10.1080/10408398.2020.1774497.
- Shoeibi, S., and M. Mashreghi. 2017. Biosynthesis of selenium nanoparticles using *Enterococcus faecalis* and evaluation of their antibacterial activities. *Journal of Trace Elements in Medicine and Biology* 39 (January):135–9. doi:10.1016/j.jtemb.2016.09.003.
- Szklarczyk, D., A. Santos, C. von Mering, L. J. Jensen, P. Bork, and M. Kuhn. 2016. STITCH 5: Augmenting protein-chemical interaction networks with tissue and affinity data. *Nucleic Acids Research* 44 (D1):D380–384. doi:10.1093/nar/gkv1277.
- Vahdati, M., and T. Tohidi Moghadam. 2020. Synthesis and characterization of selenium nanoparticles-lysozyme nanohybrid system with synergistic antibacterial properties. *Scientific Reports* 10 (1):510. doi:10.1038/s41598-019-57333-7.
- Verma, S. K., E. Jha, P. Kumar Panda, M. Mukherjee, A. Thirumurugan, H. Makkar, B. Das, S. K. S. Parashar, and M. Suar. 2018. Mechanistic insight into ROS and neutral lipid alteration induced toxicity in the human model with fins (*Danio rerio*) by industrially synthesized titanium dioxide nanoparticles. *Toxicology Research* 7 (2):244–57. doi:10.1039/c7tx00300e.
- Vikneshan, M., R. Saravanakumar, R. Mangaiyarkarasi, S. Rajeshkumar, S. R. Samuel, M. Suganya, and G. Baskar. 2020. Algal biomass as a source for novel oral nano-antimicrobial agent. *Saudi Journal of Biological Sciences* 27 (12):3753–8. doi:10.1016/j.sjbs.2020.08.022.
- Wadhvani, S. A., M. Gorain, P. Banerjee, U. U. Shedbalkar, R. Singh, G. C. Kundu, and B. A. Chopade. 2017. Green synthesis of selenium nanoparticles using *Acinetobacter* sp. SW30: Optimization, characterization and its anticancer activity in breast cancer cells. *International Journal of Nanomedicine* 12:6841–55. doi:10.2147/IJN.S139212.
- Yang, G., and S.-J. Park. 2019. Conventional and microwave hydrothermal synthesis and application of functional materials: A review. *Materials* 12 (7):1177. doi:10.3390/ma12071177.
- Zahran, W. E., S. M. Elsonbaty, and F. S. M. Moawed. 2017. Selenium nanoparticles with low-level ionizing radiation exposure ameliorate nicotine-induced inflammatory impairment in rat kidney. *Environmental Science and Pollution Research* 24 (24):19980–9. doi:10.1007/s11356-017-9558-4.

- Zambonino, M. C., E. M. Quizhpe, F. E. Jaramillo, A. Rahman, N. Santiago Vispo, C. Jeffryes, and S. A. Dahoumane. 2021. Green synthesis of selenium and tellurium nanoparticles: Current trends, biological properties and biomedical applications. *International Journal of Molecular Sciences* 22 (3):989. doi:[10.3390/ijms22030989](https://doi.org/10.3390/ijms22030989).
- Zhang, D., X-l. Ma, Y. Gu, H. Huang, and G-w. Zhang. 2020. Green synthesis of metallic nanoparticles and their potential applications to treat cancer. *Frontiers in Chemistry* 8:799. doi:[10.3389/fchem.2020.00799](https://doi.org/10.3389/fchem.2020.00799).
- Zhang, W., J. Zhang, D. Ding, L. Zhang, L. A. Muehlmann, S.-E. Deng, X. Wang, W. Li, and W. Zhang. 2018. Synthesis and antioxidant properties of *Lycium barbarum* polysaccharides capped selenium nanoparticles using tea extract. *Artificial Cells, Nanomedicine, and Biotechnology* 46 (7):1463–70. doi:[10.1080/21691401.2017.1373657](https://doi.org/10.1080/21691401.2017.1373657).